

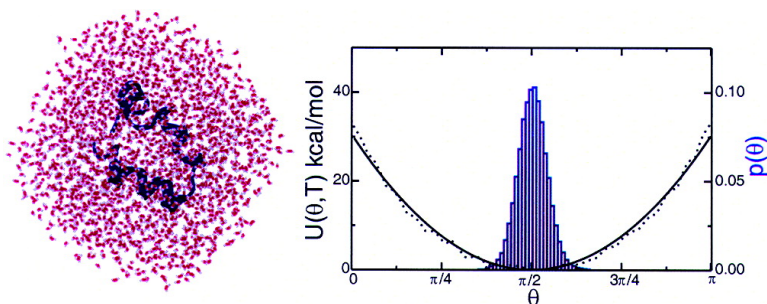
Communication

**Temperature Dependence of NMR Order Parameters and Protein Dynamics**

Francesca Massi, and Arthur G. Palmer

*J. Am. Chem. Soc.*, **2003**, 125 (37), 11158-11159 • DOI: 10.1021/ja035605k • Publication Date (Web): 22 August 2003

Downloaded from <http://pubs.acs.org> on March 29, 2009



**More About This Article**

Additional resources and features associated with this article are available within the HTML version:

- Supporting Information
- Links to the 3 articles that cite this article, as of the time of this article download
- Access to high resolution figures
- Links to articles and content related to this article
- Copyright permission to reproduce figures and/or text from this article

[View the Full Text HTML](#)

## Temperature Dependence of NMR Order Parameters and Protein Dynamics

Francesca Massi and Arthur G. Palmer, III\*

Department of Biochemistry and Molecular Biophysics, Columbia University, New York, New York 10032

Received April 13, 2003; E-mail: agp6@columbia.edu

Protein conformational dynamics have been extensively studied using NMR spectroscopy by measuring  $^2\text{H}$ ,  $^{13}\text{C}$ , and  $^{15}\text{N}$  nuclear spin relaxation rate constants.<sup>1</sup> Spin relaxation data frequently are interpreted using the model-free formalism<sup>2</sup> that parametrizes the equilibrium distributions of bond vector orientations in a molecular reference frame by generalized order parameters,  $S$ . This communication uses computer simulations of the villin headpiece helical subdomain, HP36,<sup>3</sup> to investigate the temperature dependence of internal motions of the backbone amide moiety in proteins. The potential of mean force (PMF) for the N–H bond vector is calculated from constrained molecular dynamics (MD) simulations using umbrella sampling. The PMF is found to be significantly temperature-dependent, in contrast to the temperature-independent potential energy functions that have been proposed for the interpretation of the temperature dependence of  $S$ .<sup>4–7</sup> A simple analytical expression is obtained that describes the temperature-dependent PMF. The parameters of this model are obtained from the PMF, from values of  $S$  derived from MD simulations, or from values of  $S$  derived from experiments. Proper understanding of the temperature dependence of  $S$  is essential to the use of NMR spectroscopy for investigating the role of conformational fluctuations in processes such as ligand binding and folding of proteins.<sup>1,8</sup>

The probability,  $p(\Omega)$ , of finding the N–H vector in a given orientation in a molecular reference frame is given by:

$$p(\Omega) = \exp(-\beta W(\Omega))/Z \quad (1)$$

in which

$$Z = \int \exp(-\beta W(\Omega)) d\Omega \quad (2)$$

$\beta = 1/(kT)$ ,  $\Omega = \{\theta, \phi\}$ , and  $d\Omega = \sin \theta d\theta d\phi$ .  $W(\Omega)$  represents the conformational free energy of the N–H bond vector in an orientation specified by  $\Omega$  or, in other words, the PMF acting on the N–H bond vector for various configurations of peptide and solvent molecules.

The PMF for N–H bond vectors in the  $\alpha$ -helix region of HP36 were calculated at temperatures of 273, 289, and 305 K. Umbrella sampling was used because large energy barriers may prevent an accurate sampling of the PMF in an unconstrained MD simulation and model potential energy functions differ most strongly for large angular excursions.<sup>4,5,7</sup> The PMF was assumed to be axially symmetric with  $W(\Omega) = W(\theta)$ . The resulting PMF is shown in Figure 1. The simulation protocol is described in the caption. Overall peptide motion was eliminated by translating and rotating all molecules at each time step to remove displacements of the peptide center of mass and to minimize root-mean-square deviations of the peptide backbone  $\text{C}^\alpha$  atoms from a reference configuration;<sup>9,10</sup> other approaches have been described.<sup>11</sup> At each temperature, the calculated PMF is adequately described by a parabolic potential,  $W(\theta) \propto (\theta - \theta_{\text{eq}})^2$ .<sup>12,13</sup> Assuming a linear temperature dependence of the PMF:

$$W(\theta, T) = W_0 f(\theta) [1 + \alpha(T - T_0)] \quad (3)$$

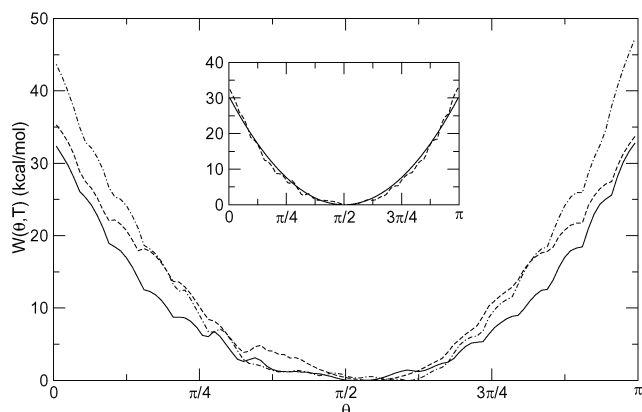


**Figure 1.** Potential of mean force for the backbone N–H bond vector of alanine 49 of HP36 at 273 K (· · · · ·), 289 K (– – –), and 305 K (–). The system consisted of the peptide, 1840 water molecules, and two chloride ions. The simulation protocol used version-27 of the potential energy function of the CHARMM program<sup>14</sup> with periodic boundary conditions, a 12 Å cutoff for evaluation of nonbonded interactions, and Ewald summation to evaluate electrostatic interactions. The equations of motion were integrated with the Verlet algorithm. A time step of 2 fs was used with coordinates saved every 100 fs. Umbrella sampling calculations were performed at each temperature using biasing potentials  $w_j(\theta) = K(\sin \theta - \sin \theta_j)^2$ , where  $K$  is equal to  $745.5 \text{ kcal mol}^{-1}$  and  $\theta_j$  is  $0, 10^\circ, 20^\circ, \dots, 180^\circ$ . The  $z$ -axis was orthogonal to the equilibrium N–H orientation. For each of the 19 windows, two simulations of 170 ps were performed. The biased histograms were processed with the WHAM method<sup>15</sup> to yield the PMF. The inset shows the PMF at 305 K (– – –) fitted with eq 3 (–). Similar fits are obtained for 273 and 289 K.

where  $\alpha = (\partial \ln W/\partial T)_{T=T_0}$  and  $f(\theta)$  expresses the dependence of PMF on  $\theta$ . The results from fitting eq 3 to the PMF are presented in Figure 1. The best fit is given by  $W_0 = 14.81 \pm 0.10 \text{ kcal/mol}$ , and  $\alpha = -0.0103 \pm 0.0002 \text{ K}^{-1}$ , for  $T_0 = 289 \text{ K}$ .

The PMF is the change in Helmholtz free energy,  $A(\theta) - A(\theta_{\text{eq}})$ , due to reorientation of the N–H bond vector from its equilibrium value,  $\theta_{\text{eq}} = \pi/2$ , which corresponds to an arbitrary choice of the state of zero energy. Over the limited temperature range of the calculations, the change in entropy,  $\Delta S(\theta)$ , can be considered constant. Thus,  $\Delta S(\theta) = -[W(\theta, T_0 + \Delta T) - W(\theta, T_0 - \Delta T)]/(2\Delta T)$  and  $\Delta E(\theta) = W(\theta, T_0) + T_0 \Delta S(\theta)$ . From the expression for the PMF given in eq 3,  $\Delta S(\theta) = -W_0 \alpha f(\theta)$  and  $\Delta E(\theta) = W_0(1 - \alpha T_0) f(\theta)$ . The results of this decomposition are shown in Figure 2.

The parameter,  $\Lambda$ , has been introduced to characterize the temperature dependence of the order parameter  $S$ :<sup>4</sup>

$$\Lambda = \frac{d \ln(1 - S)}{d \ln T} \quad (4)$$

The generalized order parameter is defined as<sup>2</sup>

$$S = \sqrt{\frac{4\pi}{5} \sum_{m=-2}^2 |\langle Y_2^m(\Omega) \rangle|^2} \quad (5)$$

where  $Y_2^m(\Omega)$  are the second-order spherical harmonics. The

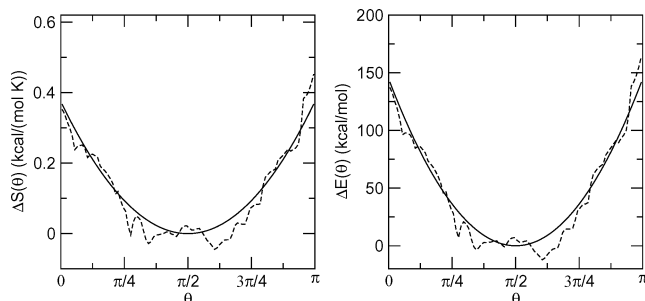


**Figure 2.** Entropic and energetic contributions to the PMF evaluated at  $T_0 = 289$  K. The dashed line depicts  $\Delta S(\theta)$  and  $\Delta E(\theta)$  obtained from the PMF. The solid line represents the entropic and energetic contributions obtained from the fit to  $W(\theta, T)$  using eq 3, respectively given by  $\Delta S(\theta) = -W_0\alpha(\theta - \theta_{eq})^2$  and  $\Delta E(\theta) = W_0(1 - \alpha T_0)(\theta - \theta_{eq})^2$ .

ensemble average  $\langle Y_2^m(\Omega) \rangle$  is equal to

$$\langle Y_2^m(\Omega) \rangle = \int d\Omega Y_2^m(\Omega) p(\Omega) \quad (6)$$

Generalizing eq 3 to  $W(\Omega, T) = W_0 f(\Omega)[1 + \alpha(T - T_0)]$  and using eqs 4–6 yields,

$$\frac{\Lambda}{\Lambda_0} = 1 - \alpha T_0 \quad (7)$$

in which  $\Lambda_0$  is the value of  $\Lambda$  calculated for  $\alpha = 0$ , i.e. for a temperature-independent potential with the same values  $W_0$  and  $f(\Omega)$ . The contribution to the heat capacity from reorientational fluctuations is given by:

$$c_p = T \frac{dS_p}{dT} \quad (8)$$

in which the conformational entropy,  $S_p$ , is given by:<sup>8,16,17</sup>

$$S_p = -k \int p(\Omega) \ln p(\Omega) d\Omega \quad (9)$$

Substituting  $p(\Omega)$  into eq 9 yields

$$c_p|_{T=T_0} = \frac{\Lambda}{\Lambda_0} c_p|_{T=T_0, \alpha=0} \quad (10)$$

Equations 7 and 10 show that  $\Lambda$  is directly related to the temperature-dependent effective potential for reorientation of the N–H bond vector. Measurements of  $S$  and  $\Lambda$  therefore provide information about the effective potential and about contributions of reorientational fluctuations to heat capacity.

MD simulations of HP36 in the absence of any constraints have been run at five temperatures, 275, 279, 289, 295, and 305 K. Values of  $S$  have been calculated from the trajectories at each temperature and used to calculate  $\Lambda$  using eq 4. The values of  $S$  and  $\Lambda$  were used to evaluate  $W_0$ ,  $\alpha$ , and  $\Lambda_0$  using eqs 5–7. Figure 3 summarizes the resulting values of  $S$ ,  $\Lambda$ ,  $W_0$ ,  $\alpha$ , and  $\Lambda_0$  for HP36. Values of  $W_0 = 11.3 \pm 2.5$  kcal/mol and  $\alpha = -0.008 \pm 0.004$  K<sup>-1</sup> determined in this manner for residue Ala 49 agree with values obtained from directly fitting the PMF. Figure 3 also shows that the distribution of  $\theta$  from the unconstrained simulations agrees with the  $p(\theta)$  obtained from the PMF, although a narrower range of  $\theta$  is sampled. Thus,  $W(\theta, T)$  given in eq 3 adequately describes the simulated unconstrained dynamics of backbone N–H bond vectors in HP36. Average values of  $\alpha = -0.011 \pm 0.006$  K<sup>-1</sup> and  $W_0 = 9 \pm 2$  kcal/mol, obtained from experimentally determined values of  $S$  and  $\Lambda$  for residues in the helices of HP36,<sup>4</sup> also agree with simulated values.

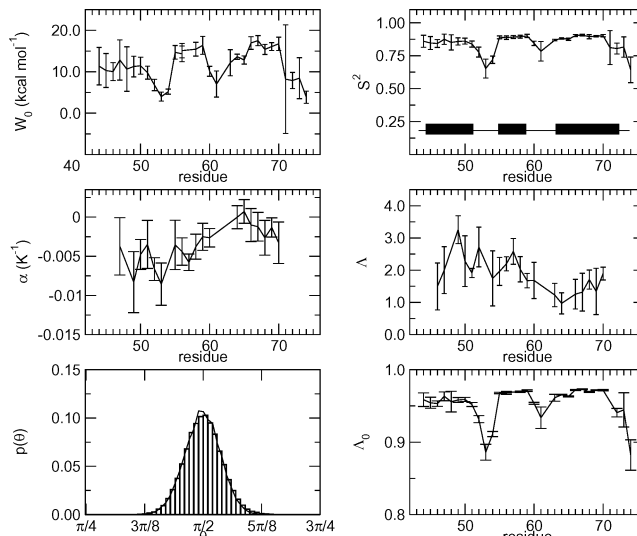


**Figure 3.**  $W_0$ ,  $\alpha$ , and  $\Lambda_0$  calculated with eq 4–7 using values of  $S$  and  $\Lambda$  obtained from five 1-ns MD simulations at five temperatures. The system consisted of the peptide, 1840 water molecules and two chloride ions. The simulation protocol used version-27 of the potential energy function of the CHARMM program<sup>14</sup> with periodic boundary conditions, a 12 Å cutoff for evaluation of nonbonded interactions, and Ewald summation to evaluate electrostatic interactions. The equations of motion were integrated with the leapfrog algorithm. A time step of 2 fs was used with coordinates saved every 200 fs. Values of  $S^2$  are shown for 289 K; as indicated by the large error bars, independent simulations have not converged for the loop between helix 1 and 2. In the same panel,  $\alpha$ -helical regions of HP36 are indicated with black boxes. The distribution of the values of  $\theta$  for the N–H bond vector of Ala 49 from these simulations (bars) is compared with the probability  $p(\theta)$  obtained from the calculated PMF (solid line) at  $T = 289$  K; for clarity only the region between  $\pi/4$  and  $3\pi/4$  is shown.

In summary, a temperature-dependent effective potential energy function for internal motion of protein backbone amide bond vectors has been developed and validated using computational simulations. The parameters  $W_0$  and  $\alpha$  that define the potential can be obtained from the experimental temperature dependence of the generalized order parameter  $S$ . Information on the effective potential is essential for studies of configurational fluctuations in proteins using NMR spectroscopy.

**Acknowledgment.** This work was supported by the National Institutes of Health Grant GM50291. We thank John E. Straub and David A. Case for helpful discussion.

## References

- Palmer, A. G. *Annu. Rev. Biophys. Biomol. Struct.* **2001**, *30*, 129–155.
- Lipari, G.; Szabo, A. J. *Am. Chem. Soc.* **1982**, *104*, 4546–4559.
- McKnight, C. J.; Doering, D. S.; Matsudaira, P. T.; Kim, P. S. *J. Mol. Biol.* **1996**, *260*, 126–134.
- Vugmeyster, L.; Trott, O.; McKnight, C. J.; Raleigh, D. P.; Palmer, A. G. *J. Mol. Biol.* **2002**, *320*, 841–854.
- Lee, A. L.; Sharp, K. A.; Kranz, J. K.; Song, X. J.; Wand, A. J. *Biochemistry* **2002**, *41*, 13814–13825.
- Prabhu, N. V.; Lee, A. L.; Wand, A. J.; Sharp, K. A. *Biochemistry* **2003**, *42*, 562–570.
- Mandel, A. M.; Akke, M.; Palmer, A. G., III. *Biochemistry* **1996**, *35*, 16009–16023.
- Akke, M.; Bruschweiler, R.; Palmer, A. G., III. *J. Am. Chem. Soc.* **1993**, *115*, 9832–9833.
- Amadei, A.; Linssen, A. B. M.; Berendsen, H. J. C. *Proteins: Struct., Funct., Genet.* **1993**, *17*, 412–425.
- Kabsch, W. *Acta Crystallogr.* **1976**, *A32*, 922–923.
- Amadei, A.; Chillemi, G.; Ceruso, M. A.; Grottesi, A.; Di Nola, A. *J. Chem. Phys.* **2000**, *112*, 9–23.
- Karplus, M.; Kushick, J. N. *Macromolecules* **1981**, *14*, 325–332.
- Prompers, J. J.; Bruschweiler, R. *J. Chem. Phys.* **2000**, *104*, 11416–11424.
- Brooks, B. R.; Brucoleri, R.; Olafson, B.; States, D.; Swaminathan, S.; Karplus, M. *J. Comput. Chem.* **1983**, *4*, 187–217.
- Kumar, S.; Bouzida, D.; Swendsen, R. H.; Kollman, P. A.; Rosenberg, J. M. *J. Comput. Chem.* **1992**, *13*, 1011–1021.
- Yang, D.; Kay, L. E. *J. Mol. Biol.* **1996**, *263*, 369–382.
- Li, S.; Raychaudhuri, S.; Wand, A. J. *Protein Sci.* **1996**, *5*, 2647–2650.

JA035605K